THE DISPATCH

Volume 3, Issue 2 | Defense Threat Reduction Information Analysis Center | June 2013

This Issue

Contact Us

dtriac@dtra.mil
or visit us at
www.dtriac.dtra.mil

From the Program Manager

Welcome! DTRA realigned DTRIAC from the J3/7 Operations/Exercise and Readiness Directorate to the J9 Research and Development Directorate, and I was designated as the Interim Program Manager (PM) for DTRIAC until a permanent PM is brought on board. I support Dr. Steven Wax, Chief Scientist, DTRA/J9ST. The J9 and J9ST look forward to having DTRIAC as part of our organization, and we plan to continue increasing awareness of DTRIAC functions and capabilities.

J9 personnel are excited to contribute articles on our various research efforts in support of DTRA's combating WMD mission. We also plan to finish the NextGen STARS development that was started under J3/7. Our goal is to improve the inclusiveness of and access to DTRIAC for the entire agency.

This issue of The Dispatch focuses on airblast phenomena. DTRA and its predecessor organizations have a long history of research in this area, and DTRA continues to perform a variety of research in this field. Some of the articles detail effects of nuclear detonation in an urban environment. Other articles describe airblast codes, which have been updated using improved modeling and methodology, and their validity in urban environments.

UPSHOT-KNOTHOLE: Mr. Inquest filming ENCORE test airblast, May 8, 1953

Please contact us directly if you ever have any questions or comments related to DTRIAC at dtriac@dtra.mil.

Thanks,

Santiago (San) Simpliciano
DTRIAC Interim Program Manager

Validation of Nuclear Airblast Codes

By: James F. Heagy, Ph.D

DTRA continues to invest in first-principle codes to predict airblast casualties and damage resulting from nuclear and large-scale conventional explosions. These first-principles codes are essential surrogates for actual nuclear detonations. One such code is the Second-Order Hydrodynamic Automatic Mesh Refinement Code (SHAMRC), developed by Applied Research Associates, Inc. (ARA) SHAMRC is specifically designed to model nonideal airblasts in environments where terrain and obstructions play significant roles, for example a nuclear detonation at ground level in a dense urban setting.

Validation of airblast codes is a necessary and important process in the code development life cycle. Results of validation studies are used to flush out "bugs," modify underlying physics assumptions, and refine implementation algorithms. One way to validate codes such as SHAMRC is to compare SHAMRC predictions (typically static overpressure and dynamic pressure) with measurements from scaled blast experiments. This method has the advantage of allowing code comparisons to recent and ongoing experiments using modern facilities and test instruments. Another validation strategy is to compare SHAMRC predictions with measurements from historical nuclear (or large-scale nonnuclear) tests. This method has the advantage of testing the code for a wider range of physical effects. In the case of SHAMRC, such effects include blast wave diffraction over large-scale terrain, thermal precursor effects, and the effects of dust injection.

DTRA tasked the Institute for Defense Analyses (IDA) to undertake the validation of SHAMRC. Their validation process includes comparisons of SHAMRC predictions with the WINDRUSH scaled urban blast experiments as well as comparisons of SHAMRC with measurements from the 1959 SMOKY nuclear test. IDA devised a comparison methodology that examines differences between model predictions and data in the context of their operational relevance; priority is given to differences in regimes where significant casualties and damage are expected to occur.

Are Airblast Codes Validated for Urban and Suburban Areas?

By: Culbert B. Laney, TASC

Two recent events dramatize the possible impacts of air blast on urban and suburban areas. On February 15, 2013, a meteor strike near Chelyabinsk in Russia created an airblast source at a height of 15 miles with a nominal yield of 470 kT TNT—about 30 times greater than the bomb dropped on Hiroshima, Japan, according to an estimate from Dr. Peter Brown and the Meteor Physics Group at the University of Western Ontario, Canada. Russian media reported that over 3,000 buildings were damaged, including over 100,000 square meters of window glass. In the final analysis, "there were no deaths and most of the 1,500 injuries were from glass…," according to *The New York Times*. While there were numerous reports of facial injuries due to glass, there were no reports of blindness—unlike earlier incidents such as the Halifax, Nova Scotia, explosion that occurred on December 6, 1917.

On April 18, 2013, a fertilizer plant in West, Texas, exploded. In the immediate aftermath, *Scientific American* reported a yield of about 1 kT TNT based on rough estimates of the stabilized height of the mushroom cloud. In addition, the United States Geological Survey estimated a ground shock equivalent to a 2.1-magnitude earthquake. Early news reports indicated that a combination of airblast, ground shock, and fire completely destroyed several buildings, damaged 50 to 60 additional buildings, killed 15 people, and injured over 200 additional people.

DTRA has sponsored development of three first-principles airblast codes: Second-Order Hydrodynamic Automatic Mesh Refinement Code (SHAMRC), Multiphase Adaptive Zoning (MAZe3), and Radiation Adaptive Grid Eulerian (RAGE). DTRA recently initiated three independent peer reviews conducted by Exelis Inc., the Institute for Defense Analyses (IDA), and Engineer Research and Development Center (ERDC) to evaluate the performance of such codes in urban areas. For consistency and to limit costs, all three peer reviews focus on a single first-

Are Airblast Codes Validated for Urban and Suburban Areas? *(continued)*

principles code, SHAMRC. The first peer review, conducted by Exelis, concluded in September 2012. The other two peer reviews are still in an early stage.

To give a sense of the outcomes so far, Exelis validated SHAMRC against test results for a two-dimensional rectangular block in a shock tube. Exelis observed significant modeling errors on the top face of the block. In a grid refinement study, the modeling error increased rather than decreased as the number of grid points increased, confirming an observation first made by BRL in 1995. As a possible explanation, SHAMRC may slightly mis-locate or mis-size the corner vortex from the block's leading edge, causing it to incorrectly overlap a pressure sensor. However, since the test results include only face-centered pressure-time histories and not offset pressure taps or flow structures such as vortices, it is difficult to positively confirm this theory.

Jiang and Takayama noted that it is "not sufficient to compare numerical solutions with a limited set of point measurements from experiment … The validation has two aspects: one is a check on numerical values and the other is a check on characteristic flow structures" [1] such as vortices, slipstreams, terminators, shock fronts, and so forth. Judged by this standard or even by the looser standard of overpressure-time history, first-principles models may experience serious difficulties with even very simple model problems relevant to airblast in urban and suburban areas.

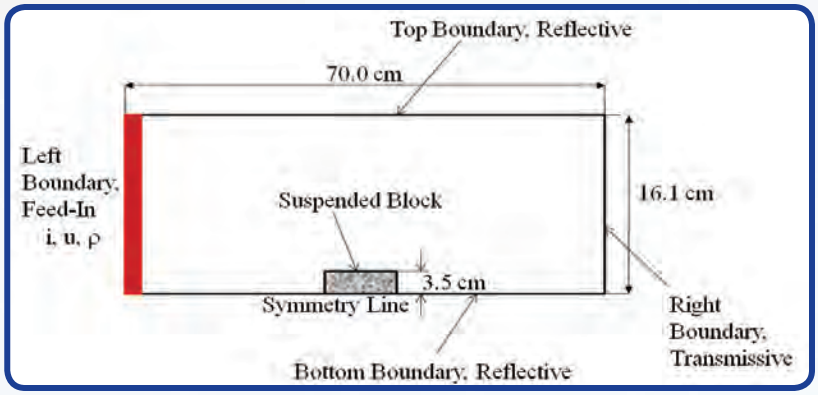

Schematic of SHAMRC solution set-up for a suspended block in the test section of a shock tube (Exelis Inc.)

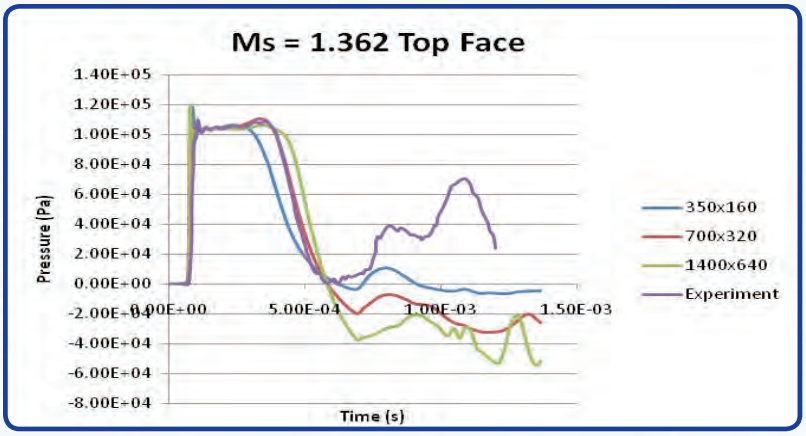

SHAMRC solutions at three different mesh sizes for M_s = 1.265 with comparisons to the experimental data provided for the top face of a suspended block in the test section of a shock tube (Exelis Inc.)

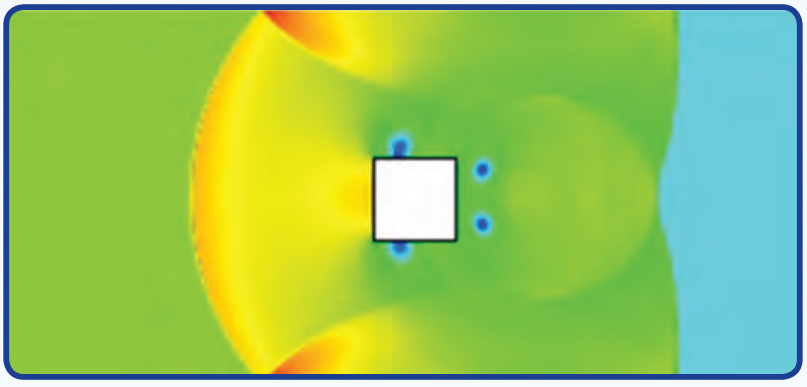

Overpressure contour plot for the modeling domain at t = 0.00120s for M_s = 1.362 (Exelis Inc.)

References

1. Jiang Z. and K. Takayama, "An Investigation into the Validation of Numerical Solutions of Complex Flowfields," *Journal of Computational Physics* 151 (1999): 479-497

Recent SHAMRC Code Improvements for Blast Modeling

By: Joseph Crepeau, Raymond Bell, Applied Research Associates, Inc.

Second-order Hydrodynamic Automatic Mesh Refinement Code (SHAMRC) is a finite-difference computational fluid dynamics (CFD) code (2D/3D, serial/parallel) used extensively by government agencies to investigate high explosive (HE) and nuclear blast phenomena[1]. SHAMRC is second-order accurate in both space and time and is fully conservative of mass, momentum, and energy. It is fast because it employs a structured Eulerian grid and efficient due to the use of the SRCLIB code preprocessor. SHAMRC capabilities include multiple geometries; nonresponding and responding structures; two-phase flow with interactive, drag-sensitive particles; several atmosphere models; multiple materials; a large material library; HE detonations; a variable coefficient K-ε turbulence model; water and dust vaporization; and a predictive metal and gaseous afterburn model.

A criticism of SHAMRC was that it was a purely hydrodynamic code and did not have material strength. Recently, Applied Research Associates, Inc. (ARA) added a material group interface tracker and material strength capability to SHAMRC. The material interface tracker (MIT) algorithm (a requirement to properly treat material strength in an Eulerian code) and strength model in SHAMRC are based on the models implemented in CTH[2], which includes the state-of-the-art Sandia Modified Young's Reconstruction Algorithm (SMYRA)[3]. The addition of material strength to SHAMRC allows users to apply SHAMRC to a wider range of blast-related problems. Some examples of these types of problems include cased charge breakup, explosive storage magazine response to internal detonation, and building response to blast from nuclear detonations in urban terrain.

Material Group Interface Tracker Algorithm

The MIT algorithm implemented in SHAMRC, called the SHAMRC Interface Reconstruction Algorithm (SHIRA), uses an improved version of SMYRA to track interfaces and adds the concept of material groups to classify materials with similar strength properties in the same group. This concept allows materials without strength to mix, as they would normally, but keeps them separate from those with strength. SHIRA tracks individual material energies for each material, allowing hot gases to be in contact with cold metals without the unrealistic energy transfer from the gases to the metal. In groups containing more than one material, the materials in that group are allowed to come to temperature and pressure equilibrium. The cell pressure is defined as the volume fraction weighted pressure of all groups in the cell.

Another significant difference between SHIRA and SMYRA is the use of preferential fluxing during the HE detonation process. This preferential fluxing is accomplished by modifying the group advection order, causing all materials other than detonated explosives to have a higher priority to be fluxed out of the zone. Once the detonation is complete, the preferential fluxing is ignored, the burned explosive materials are returned to the original group, and the material order is again a function of the volume fractions upstream and downstream of the donor cell.

Material Strength

SHAMRC is generally applied in regimes of extremely high pressures and energies, where materials behave as a fluid, or at lower pressures where material response in unimportant. It is the area between these two regimes, where the effect of material strength becomes significant, that is of interest. The material strength model implemented in SHAMRC closely mirrors the model currently implemented in CTH, with appropriate adjustments due to differences in the differencing scheme between the two codes.

Stress deviator variables, proportional to the stresses in the cells, are included for each computational cell. At appropriate points in a computational cycle, cell velocities and energies are updated due to the effect of these deviators. A void-volume-fraction variable is included for each computational cell to account for material fracture.

Currently, metal materials use a von Mises model to determine the current cell yield. Geologic materials (sand, concrete, rock, etc.) use a geologic model. The Johnson-Cook model is also available for many metals. All materials are also subject to fracture once the tension (measured by a negative material pressure) exceeds the fracture strength of the material. Once fractured the material density is re-set to ambient and the volume fraction deficit is added to the void volume fraction for the cell.

Recent SHAMRC Code Improvements for Blast Modeling *(continued)*

Verification and Validation (V&V) and Code Calibration Calculations

A number of calculations were run to verify and validate, and calibrate the models implemented in SHAMRC. Figure 1 shows the outline of steel density contours for a 2D axisymmetric SHAMRC calculation of the detonation of a cased weapon at 500 μs. The images are of three calculations of the same scenario. The left image is from a calculation without an interface tracker, the middle image is with an interface tracker but no material strength, and the right image is with a material interface tracker and material strength. The material interface tracker does an excellent job of keeping the steel from diffusing into the explosive products and into the surrounding air. With the material strength model, the case breaks at key stress points, as seen near the tail (top of the image) of the weapon.

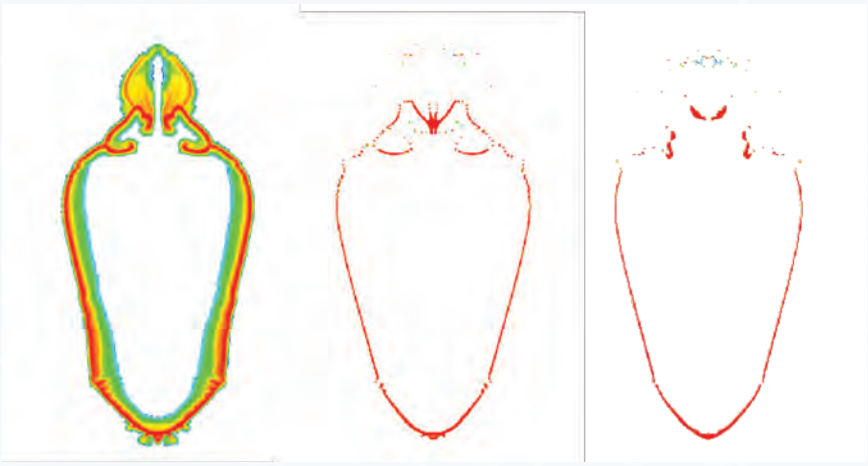

Figure 1. Comparison of steel density contours at 500 μs from SHAMRC calculations of the case expansion from a weapon without MIT and strength (left), with MIT and no strength (center) and with MIT and strength (right) (ARA, Inc.)

Other calculations run for code validation include: (1) Taylor Anvil, (2) copper ball impacting a steel plate, (3) long tungsten penetrating rod, (4) explosively formed penetrator, and (5) a buried charge in sand. Results from each of the SHAMRC calculations were compared with corresponding CTH calculations for calibration purposes. All SHAMRC calculations produced results that are in very good agreement with the CTH results. Figure 2 shows a comparison of results from Taylor Anvil calculations between SHAMRC and CTH. The Taylor Anvil problem involves an aluminum rod impacting an infinitely strong plate at 275 m/s. The profile of the aluminum cylinder at the end of the impact calculated by SHAMRC is of interest and is in excellent agreement with the CTH results. Results from the V&V and calibration calculations give strong confidence in the MIT and material strength models implemented in SHAMRC and in their applicability to emerging problems of interest.

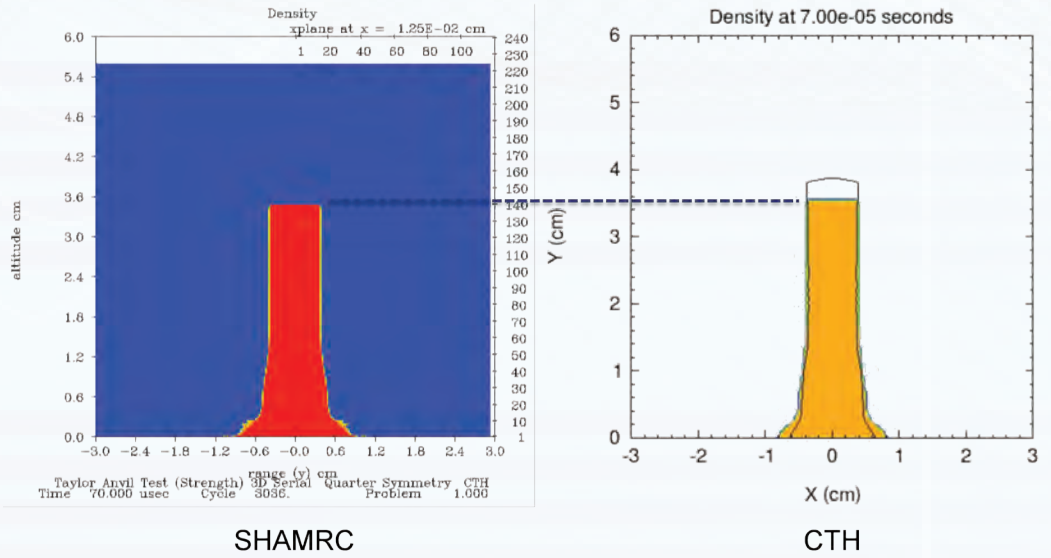

Figure 2. Comparison of aluminum rod deformation between SHAMRC and CTH at 70 μs (ARA, Inc.)

References

1. Crepeau, J.E., Needham, C.E., Hikida, S., Happ, H.J., "Second Order Hydrodynamic Automatic Mesh Refinement Code (SHAMRC): Volume I, Methodology," November 2011.
2. Bell, R.L. et al, CTH User's Manual and Input Instructions version 7.1, Sandia National Laboratories, Albuquerque, NM, 2006.
3. Bell, R.L., Hertel, E.S., "An Improved Material Interface Reconstruction Algorithm for Eulerian Codes", SAND92-1716, Sandia National Laboratories, Albuquerque, NM, 1992.

Building Effects on Cloud Rise from Nuclear Detonations in Urban Terrain

By: Charles Needham, Applied Research Associates, Inc

A small nuclear detonation (1–10 kT) in an urban environment does not produce a fireball. Over a flat, desert surface, the fireball from a 1-kT surface burst would reach approximately 125 m in radius or 250 m in diameter. There are very few locations in urban areas where a structure would not be encountered within 125 m of the detonation point. An 8-kT detonation produces a fireball with twice the dimensions of a 1-kT fireball. The blast wave reflects from the surface of structures and pushes the hot gasses back toward the burst point. The urban fireball expands down streets and is forced upward by the reflected shocks. Figure 1 shows two views of an 8-kT fireball in a realistic urban environment. Note that the horizontal diameter is about half of the vertical radius. The shock also has a greater vertical radius than horizontal.

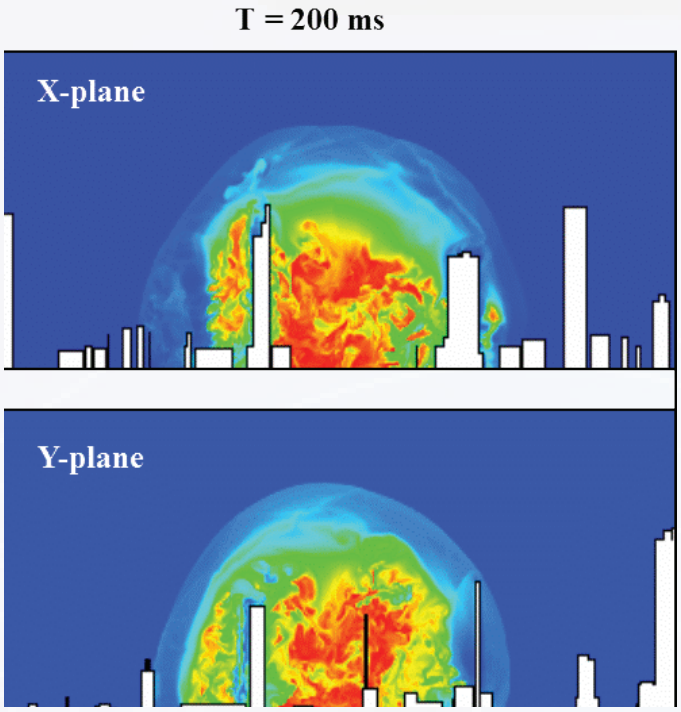

Figure 1. 8-kT surface burst in a realistic urban environment (ARA, Inc.)

As the shock engulfs a building, strong vortices are formed at the edges of the structure. The vortices induce mixing of the hot gasses with ambient air. The hot material of what would be called a fireball is not a ball at all—arms of hot debris extend down streets. Vortices continue to rotate at the edge of every building encountered causing entrainment and rapid cooling of the hot material while trapping radioactive debris. The larger surface area of the hot material enhances radiative cooling and mixing, thus further cooling the hot material. At 5 s, the maximum temperature in the 1-kT urban fireball is less than 2,000 K. Figure 2 shows the 1,000-K surface for the 1-kT detonation. There is a huge change in surface area and many vortices that have separated from the inner region.

The reflected shock waves from the buildings closer to the detonation tend to confine the radial expansion of the fireball, thus causing enhanced vertical growth. At 5 s, the urban "fireball" has risen about 50% higher than the fireball over an ideal surface. The images in Figure 3 show the geometries of the high-temperature regions for detonations over an ideal surface (left) and in an urban environment (right). Note that the peak temperature in the fireball over the ideal surface is about 9,000 K, while the peak temperature in the urban hot region is less than 2,000 K.

Figure 2. 1,000-K surface for 1 kT in urban environment (ARA, Inc.)

The rise of the urban hot region has already slowed and the buoyancy of the urban region is significantly less than that of the fireball over an ideal surface. The drag force on the urban hot region is increased because of the larger surface area. The higher drag force, combined with the lower buoyancy means that the stabilization altitude for the urban fireball will be significantly lower than for a fireball over an ideal surface.

For near-surface detonations, the overall effect on the rising fireball is that the rise velocity after 5 s is slow-

Building Effects on Cloud Rise from Nuclear Detonations in Urban Terrain *(continued)*

er, and the afterwinds caused by the rising fireball will be lower. The urban fireball will not rise as far as the fireball over an ideal surface. The afterwinds will not draw as much material into the stem to mix with the radioactive debris, and that debris will not be lofted to as high an altitude as that over an ideal surface. In addition, unlike the ideal surface case, some of the radioactive debris in the urban detonation is trapped near the ground by the vortices created by the buildings and will not be lofted more than a few hundred feet. This trapped debris will be well mixed with urban debris and cause heavy but localized fallout. The stabilization altitude of the cloud will be significantly lower than for the ideal surface, and the high-altitude winds will not have a large effect on carrying radioactive fallout away from ground zero.

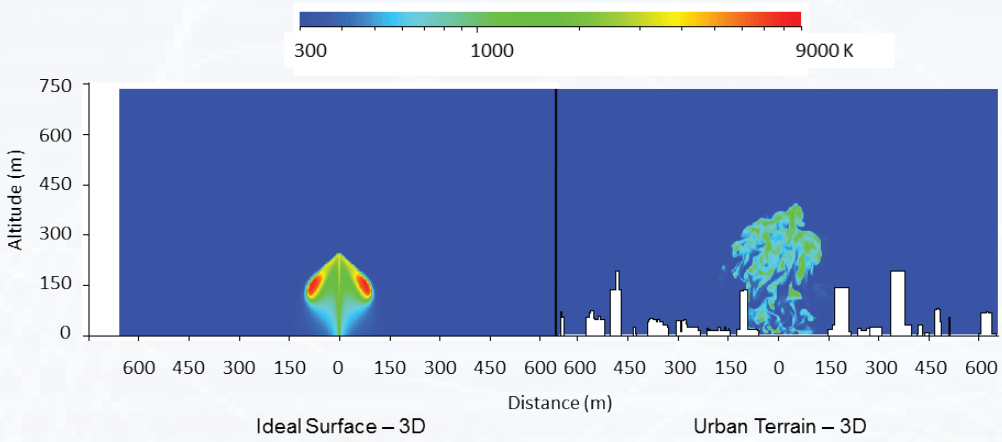

Figure 3. Comparison of temperature distribution for 1 kT over an ideal surface and in urban terrain (ARA, Inc.)

Building Effects on Airblast from Nuclear Detonations in Urban Terrain

By: Charles Needham, Applied Research Associates, Inc.

The detonation of a relatively small nuclear device (1–10 kT) in an urban environment results in blast characteristics that are significantly different from any detonation phenomena observed at either the Nevada Test Site (now known as the Nevada National Security Site) or the Pacific Proving Grounds. In an urban environment, the blast wave is reflected and refracted by multiple structures. Some of the structures provide "shadowing" for other nearby structures; some of the structures receive enhanced loading caused by reflected shocks from nearby structures.

In an urban environment, the buildings on either side of the streets cause reflection of the shock front back into the street. The streets act as three-sided shock tubes thus funneling the blast wave along the streets. Because the blast wave energy is restricted in its expansion in some directions by the structures, more energy is directed upward and away from the near ground structures. The distribution of the pressure at the shock front on the ground is, therefore, not circular but tends to extend along streets and alleyways and can be reduced along radials that pass regions with structures.

Figure 1 compares the overpressure as a function of distance from a 1-kT surface burst. The ideal (red) line represents the peak pressure for a flat, unobstructed plane. The purple squares represent the peak overpressure down radially aligned streets, and the blue diamonds represent the peak overpressures along other radials. The enhanced overpressures (those above the ideal line) are most likely caused by reflections from nearby structures. The blue diamonds below the ideal line are the result of shadowing from nearby structures.

As the overpressures fall below 1 bar (~ 15 psi), they tend to fall on or below the ideal curve. This is caused by the reduction in energy traveling radially, because more energy has been diverted upward by the reflections closer to the detonation point.

Building Effects on Airblast from Nuclear Detonations in Urban Terrain *(continued)*

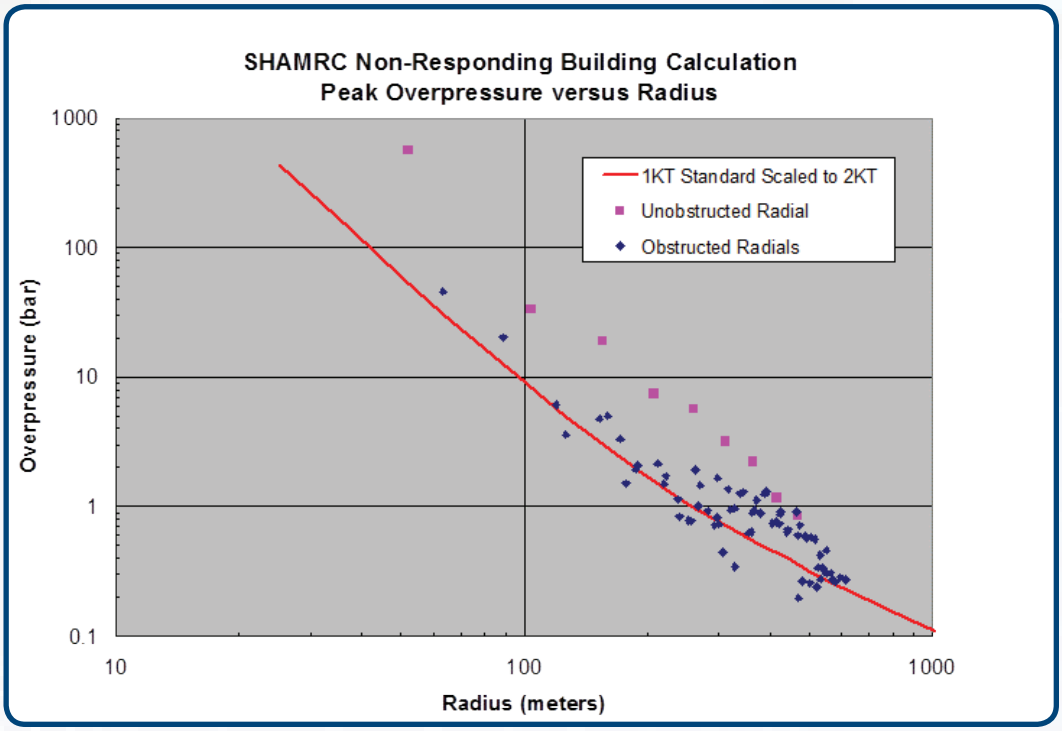

Figure 1. Urban pressure distribution along different radials (ARA, Inc.)

While the overpressure is drastically changed by the presence of buildings, the dynamic pressure is modified even greater in comparison to the ideal. The dynamic pressure is stagnated at each encounter with a building and is enhanced along streets and alleys. There are regions of nearly complete stagnation (no dynamic pressure) in regions that would have very high dynamic pressures over an ideal surface. The high dynamic pressures and dynamic impulses aligned with streets will move any loose objects such as cars, trucks, mailboxes, or sidewalk stands hundreds of feet. Cars will be piled on top of one another and block roads and access to buildings closer to the detonation point.

Many recent calculations have been criticized because they assume the buildings are nonresponding and perfectly rigid. The argument for this assumption is that the materials from which the structures are made have a density that is at least 2,000 times the density of air. This means that when a shock wave strikes a structure, the air will move 2,000 times farther than the structure in the same time interval. Thus while the building is moving 1 cm, the shock has moved more than 20 m, and the energy lost from the shock is a small fraction of 1% of the blast energy.

As an example of this behavior, an experiment was conducted at the Ernst Mach Institute in Freiburg, Germany, in which a model house was constructed of steel and exposed to a blast wave in a shock tube. Several shadowgraph pictures were taken as the shock wave engulfed the structure. Reflections from the walls and roof could be readily identified. A second model house was constructed from balsa wood using the same dimensions as the steel house and exposed to the same blast pressure.

When the shadowgraph pictures were compared, no distinction could be made between the steel and balsa wood shock reflections. The balsa wood model did not measurably move over the entire time of the shock interaction with the structure.

Another series of experiments[1,2], in the United Kingdom, were conducted with a model city built from solid concrete buildings. Pressure gauges monitored the loading at many points on buildings throughout the city. A high-explosive charge was detonated at a height of burst such that the Mach stem would be higher than the buildings as it passed over the model city. The experiments were criticized for using nonresponding structures. Therefore, the city was carefully reconstructed of thin mirror glass on light metal frames with the gauges installed at the same locations as the concrete city, and the experiments were repeated.

Building Effects on Airblast from Nuclear Detonations in Urban Terrain *(continued)*

Figure 2 shows overpressure traces from four locations within the city. First note that there is no difference in arrival time at any of the locations. The upper left waveforms (B89F) are from the front of a building near the farthest distance from the detonation. The waveforms on the upper right (B88B) were taken on the back of a building directly in front of B89. The waveforms on the lower left were from the roof of a building near the center of the city. The lower right waveforms are from the front of the building closest to the detonation. The red curves are from the concrete buildings and the blue curves are from the mirror glass buildings.

There is no appreciable difference between the waveforms. When all of the measured overpressure waveforms were compared, half of the gauges from the glass buildings were higher than those from the concrete buildings and half were below by about the same amount. Furthermore, the impulses showed the same relative amplitudes. The thin mirror glass corresponds to about an 8-inch-thick concrete wall at full scale, so this is indeed a realistic scale for responding buildings.

In conclusion, the blast overpressure in an urban environment is generally higher than for the free field. This is caused by reflections from buildings and funneling of energy down streets. For free field overpressures above approximately 5 psi, the urban pressures are nearly always higher at the same range. As the overpressures drop below about 2 psi, there are relatively more occurrences of overpressures below the ideal surface curve, but the majority of points are above the ideal curve. The approximation of using perfectly reflecting, nonresponding buildings has been proven true by multiple experiments.

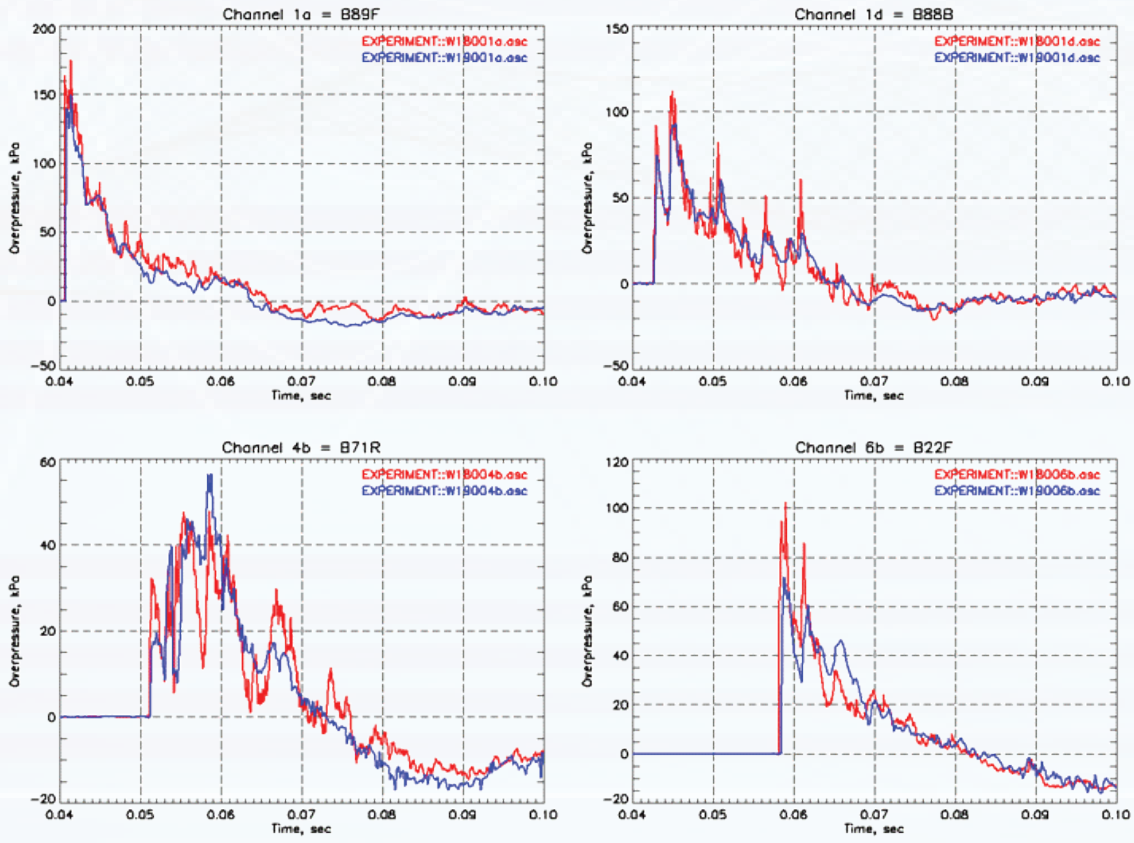

Figure 2. Comparisons of pressure records for concrete and mirror glass structures[1]

References

1. Martin, A.J., "WINDRUSH 18 – Multi-Storey Complex Flowfield Pressure Calculation," AWE Report Number AWE/DWE31/02/015; SSM/P724, February 2002 (unpublished).
2. Hunt, S., et al., "WINDRUSH High Explosive Tests," AWE (unpublished).

Modeling Nuclear Blast in Urban Terrain with NucFast

By: Charles Needham, Joseph Madrigal, Applied Research Associates, Inc.

NucFast is a 3D, fast-running, geographic information system (GIS)-based engineering-level model to determine blast, thermal, and related effects from a nuclear detonation in urban terrain. The airblast environment model is the primary model that feeds structural damage and collapse prediction of buildings, rubble pile calculation, injuries due to secondary debris (including glass breakage), and debris accumulation. The NucFast airblast model uses the DNA Nuclear Blast Standard[1], hereafter referred to as the Standard, for the basic blast parameter definition. The Standard has been adopted by the international standards committee as the airblast standard.

The Standard defines the pressure, density, and velocity as a function of radius for a 1-kT nuclear detonation in a sea-level atmosphere at any given time after detonation. It is valid from a radius of approximately 10 m to very large distances (more than an Earth circumference). Both yield scaling and atmospheric scaling can be used to represent yields from approximately 100 tons to 100 MT and from sea level to approximately 10-km altitudes. Further scaling adjustments can be made to extend the altitude of validity when needed.

To calculate a parameter time history, the Standard is called at a sequence of times at a single radius. An example is given in Figure 1 for construction of an overpressure-time history at a radius R. The Standard is called at the sequence of times t_1 to t_4 and the pressure at position R is calculated at each time. At time t_1, the shock has not reached the position R, and ambient atmospheric pressure is returned. At time t_2, the shock front has just arrived at the point R, and the peak shock pressure is returned. At t_3, the value of the pressure at point R is returned, and at t_4, a pressure below ambient is returned. The waveform is then constructed by joining the calculated pressures with a smooth curve. This process can be used to define any blast parameter as a function of time at a given point. To construct a parameter as a function of distance at a given time, the Standard is called at the same time for a series of radii.

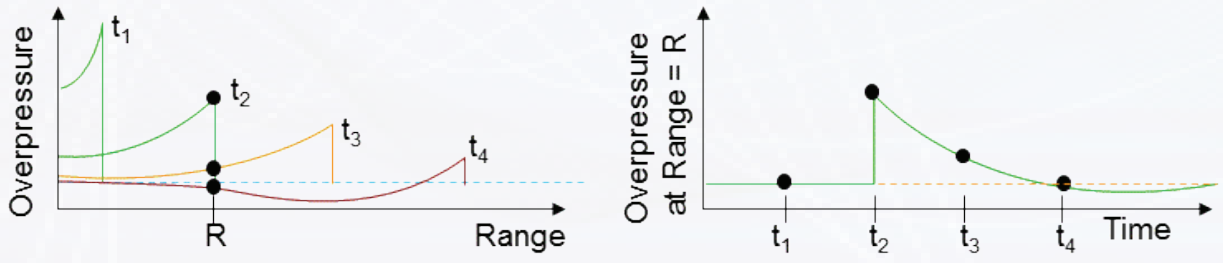

Figure 1. Construction of a time history from the nuclear standard (ARA, Inc.)

To calculate the effects of reflections from the ground an image burst algorithm is used. The surface is represented by an image burst (Figure 2) of the same yield, positioned at the same distance from the surface but on the opposite side from the reflecting surface. The low-altitude multiple burst (LAMB) Addition Rules[2] are used to add the effects of the actual burst, and the image burst at points of interest.

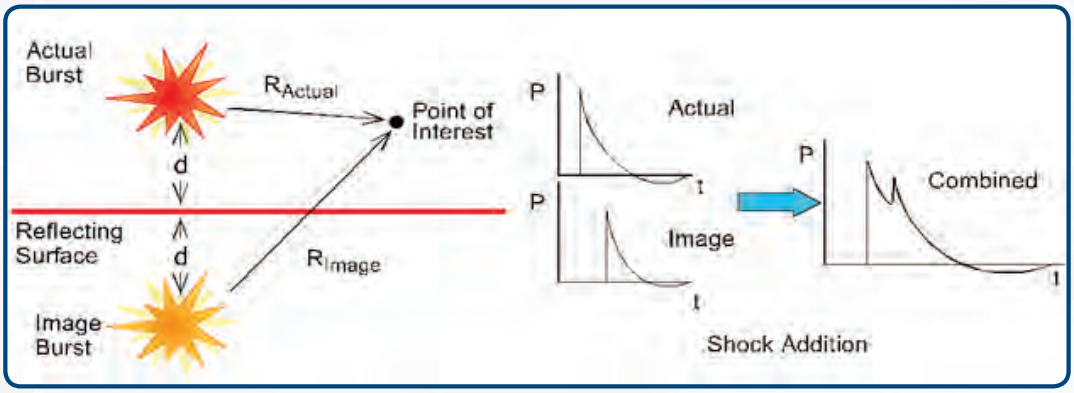

Figure 2 Image burst construct (ARA, Inc.)

Modeling Nuclear Blast in Urban Terrain with NucFast *(continued)*

To describe the blast parameters from multiple shock waves, nonlinear summation rules (called the LAMB Addition Rules) are applied using the following conservation equations of mass, momentum and energy.

Conservation of Mass

$$\rho = \rho_0 + \sum_{i=1}^{n} \Delta\rho_i$$

Conservation of Momentum

$$\rho\vec{u} = \sum_{i=1}^{n} (\rho_0 + \Delta\rho_i)\vec{u}_i$$

Conservation of Energy

$$P = P_0 + \sum_{i=1}^{n} \left[\Delta P_i + 0.5(\rho_0 + \Delta\rho_i)|\vec{u}_i|^2\right] - 0.5\frac{|\rho\vec{u}|^2}{\rho}$$

In these equations, ρ_0 is the ambient density at the point of interest, P_0 is the ambient pressure at the point of interest, $\Delta\rho_i$ is scaled shock overdensity of the i_{th} burst, ΔP_i is the scaled shock side-on overpressure of the i_{th} burst, $\vec{u}_i$ is the scaled shock velocity of the i_{th} burst, ρ is the combined shock density, P is the combined shock pressure, and $\rho\vec{u}_i$ is the combined shock momentum.

When the blast encounters objects in the scene (buildings in our case), we are interested in various parameters that when combined, define blast environments for blast loads acting on building surfaces. These parameters include peak side-on overpressure, total side-on overpressure impulse, peak dynamic pressure, and the total dynamic impulse, the shock front velocity, as well as the orientation of the resultant particle velocity for the blast. With peak side-on overpressure, dynamic pressure, peak reflected pressure, positive phase duration, and clearing time, we can estimate building surface loading that can lead to failure. The clearing time governs the duration of the reflected pressure acting on the surface. This parameter accounts for the time required for the effects associated with the edges of the building to work their way to the point of interest and relieve the reflected pressure.

Building interaction generally reduces the blast loads behind buildings due to diffraction of the blast waves around the building and increases the loads in front of buildings due to reflections off the buildings' vertical surfaces. The blast wave propagation from a burst point to an evaluation point may turn one or two corners of a building (assuming rectangular buildings) to reach an evaluation point. The equation in Figure 3 is used to calculate the incident pressure P_I for an evaluation point behind a building. R_1 is the distance to the first turning point, R_2 is the distance from R_1 to the second turning point, and R_3 is the distance from the second turning point to the evaluation point. The diffraction angles θ and ø are the turning angles evaluated at each of the turning corners. These parameters further reduce the pressure on the backside of the building by increasing the distance at which the pressure is evaluated by the sine of the angle through which the shock must turn. Applying this method produces a shadow behind the building that would eventually continue infinitely unless additional algorithms are employed to restrict the distance to the point by the characteristic length of the building. This shadow is linearly reduced to zero between three to four times the characteristic length of the building (building dimensions and height of burst are considered).

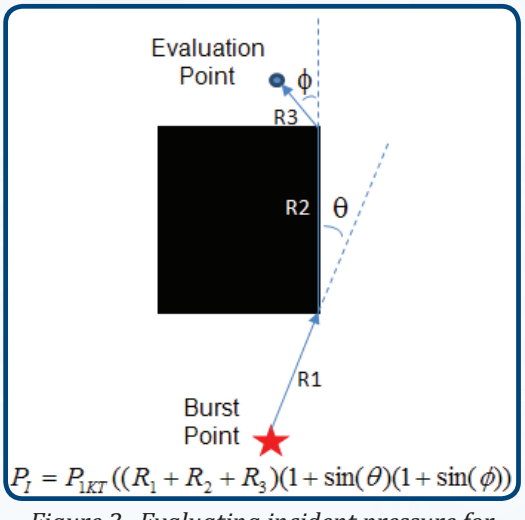

Figure 3. Evaluating incident pressure for point not in burst point line of sight (ARA, Inc.)

DTRIAC Collection Additions

DTRA Technical Reports

DTRA-TR-09-14, Evaluation of Generic 3X Upper Bound Factor Used in Reconstructing External Gamma Doses to Military Participants at Atmospheric Nuclear Weapons Tests

This report discusses the adequacy of a generic 3X upper bound factor used by the Defense Threat Reduction Agency, Nuclear Test Personnel Review in reconstructing external personnel gamma doses. Comparisons are performed between reconstructed doses with relevant film badge readings in evaluating the adequacy of applying a 3X upper bound factor to reconstructed mean doses or point estimates of doses with no uncertainty. The use of the 3X upper bound factor was usually found adequate in cases of land exposure in either the Nevada Test Site or Pacific Proving Ground. In the case of shipboard exposures in the Pacific Proving Ground, less adequacy was noted, and further investigation was recommended. Finally, a recommendation was made that doses to unbadged shipboard personnel should be assigned on the basis of badge readings for other participants on that ship, rather than a reconstructed dose.

DTRA-TR-09-15, Derivation of Effective Resuspension Factors in Scenarios for Inhalation Exposure Involving Resuspension of Previously Deposited Fallout by Nuclear Detonations at Nevada Test Site

This report presents an evaluation of inhalation doses in scenarios for exposure of military participants at atmospheric nuclear weapons tests at the Nevada Test Site that involved unusually high resuspension of radionuclides in previously deposited fallout by the thermal pulse or blast (shock) wave produced in an aboveground detonation. The purpose of this evaluation was to determine values of a resuspension factor (defined as the ratio of the concentration of resuspended radionuclides in air above ground to the areal concentration on the ground surface) that should be assumed in those scenarios to ensure that point estimates of inhalation dose obtained in dose reconstruction would be credible upper bounds, i.e., at least upper 95% credibility limits.

DTRA-TR-12-045, Characterization of the Radiological Environment at J-Village during Operation Tomodachi

This report presents a characterization of the radiological environment during Operation Tomodachi at J-Village, a facility located 12.5 mi (20 km) south of the Tokyo Electric Power Company's (TEPCO) Fukushima Daiichi Nuclear Power Station (FDNPS). The accident at FDNPS following the earthquake and tsunami on 11 March 2011 in Japan resulted in releases of radioactive materials into the environment. TEPCO used J-Village as a staging area for emergency response and cleanup. Individuals affiliated with the U.S. Department of Defense visited J-Village during Operation Tomodachi. The data presented in this report include personal dosimetry and internal monitoring results for DoD-affiliated individuals who visited J-Village, as well as external exposure rate measurements and the results of air soil, and vegetation sampling at or nearby the site. Guidelines for use of the data in future radiation dose assessments are also provided.

DTRA-TR-12-54, Engineering Methodology Report, Single-Degree-of-Freedom Component, Vulnerability Assessment and Protection Option

The Single-Degree-of-Freedom (SDOF) component adds the capability for SDOF analyses on individual building components. Higher fidelity responses can be attained using this component than are otherwise provided by typical Pressure-Impulse (P-I) diagram damage calculations.

DTRA-TR-12-55, Engineering Methodology Report for Vulnerability Assessment and Protection Option (VAPO) Multi-Hit Glass Penetration (MHGP) Injury Prediction Version 4.0

This document represents the Engineering Methodology Report Vulnerability Assessment and Option (VAPO) Multi-Hit Glass Penetration (MHGP) Injury Prediction Task. The purpose of this task is to use the knowledge gained from previous glass penetration projects to integrate the MGHP model into the VAPO code. The objective of this effort is to port the MGHP model into a model usable by the VAPO code. This document covers the background of MHGP and describes the inner workings of the software.

DTRA-TR-12-56, Engineering Methodology Report Single-Degree-of-Freedom Component Vulnerability Assessment and Protection Option Version 4.0

The single-degree-of-freedom (SDOF) component adds the capability for SDOF analyses on individual building components. Higher fidelity responses can be attained using this component than are otherwise provided by typical pressure-impulse (P-I) diagram damage calculations.

DTRA-TR-12-57, Engineering Methodology Report Glass Injury Prediction Module Vulnerability Assessment and Assessment and Protection Option, Version 5.0

The Glass Injury Prediction (GIP) Module integrates three external codes for the prediction of human injury due to glazing hazards from airblast. The GIP Module manages and performs three separate functions: (1) prediction of window glazing breakage due to airblast; (2) prediction of the hazard environment from the glazing debris; and (3) prediction of human injury caused by blunt trauma and glass shards penetration of the body. For building exposed to external blasts, the module outputs the UK Hazard Level associated with each room and optionally the injury category for discrete points within the exterior rooms of buildings.

DTRA-TR-12-58, Engineering Methodology Report, BICADS, Vulnerability and Protection Option Version 5.0

The Building Injury Calculator and Databases (BICADS) component provides an engineering methodology for the prediction of human injury inside buildings. This component integrates external code from Baker Engineering and Risk Consultants (BakerRisk) to perform the injury calculations. BICADS leverages decades of empirical data and analytic simulations to correlate human injury with structural damage, glazing damage, and interior component debris.

DTRA-TR-12-59, Engineering Methodology Report, Single-Degree-of-Freedom Component, Vulnerability Assessment and Protection Option, Version 5.0

The single-degree-of-freedom (SDOF) component adds the capability for SDOF analyses on individual building components. Higher fidelity responses can be attained using this component than are otherwise provided by typical pressure-impulse (P-I) damage calculations.

DTRIAC Collection Additions *(continued)*

DTRA-TR-12-60, Engineering Methodology Report, Advanced Automated Structural Designer (AASD), Vulnerability Assessment and Protection Option Version 5.1

The purpose of the Advanced Automated Structural Designer component is to modify a building model to achieve compliance with accepted design standards. The component supports numerous scenarios. One is the creation of "auto-designed" building model components during the model creation process. Another is the modification of sampled building model components to ensure that sampled structures are structurally sound and consistent with accepted design standards.

DTRA-TR-12-61, Engineering Methodology Report, CEDAW Model, Vulnerability Assessment and Protection Option Version 5.1

The CEDAW component as implemented in VAPO serves as the default P-I damage model on individual building components. This report discusses the CEDAW Model. The structural elements Module Engineering Methodology report (4) documents the other models that comprise the Structural Elements Module (SEM). Refer to the Component Explosive Damage Assessment Workbook (CEDAW) Methodology Manual V1.0(3) for more information regarding the design information about this model.

DTRA-TR-12-62, Engineering Methodology Report, Structural Collapse (Buildings), Vulnerability Assessment and Protection Option Version 5.1

The Load Path Collapse, Structural Analysis Module, and ProCAT models predict secondary collapse damage which results from initial blast damage to buildings. These models are necessary in order to analytically estimate the effects of munitions on targets beyond the immediate response of structural members directly exposed to blast loads. The Load Path Collapse module (LPC) predicts collapse damage by evaluating the ability of structural members in a damaged target to support gravity loads after the removal of members damaged by blast. The methodology approximates strength demands of the structure's resisting elements using uncoupled element stiffnesses while assuming a vertical load path to the foundation.

DTRA-TR-13-4, Vulnerability Updates for PDCALC

This report covers improvement to vulnerability models and methodologies for three different target types relevant to PDCALC: urban/industrial structures, personnel vulnerability, and deeply buried tunnels. The improved models for urban/industrial structures have been updated to consider updated airblast loading of structures, as well as the explicit treatment of the response of structures to an overhead burst. A new vulnerability reporting format for these structures known as a 2-VNTK is discussed. Also covered in this report is an analysis of ten personnel vulnerability tables which experienced large differences between PDCALC 7.2.3 and PDCA:C 7.3. Recommendations are made for recalculation of seven of these tables for PDCALC 8.0. Lastly, SAIC's support to the improved ground shock VN (IGVN) program is discussed.

DTRA-TR-13-5, Updating the Physical Vulnerability System for Urban Industrial Targets

This report covers improvement to vulnerability models and methodologies for urban/industrial structures. The models have been updated to consider updated airblast loading of structures as well as the explicit treatment of the response of structures to an overhead burst. A new vulnerability reporting format for these structures known as a 2-VNTK is discussed.

DTRA-TR-13-6, Vapor Growth of Mercuric Iodide Tetragonal Prismatic Crystals

The mercuric iodide project at the SMART Laboratory at Kansas State University sought to understand the role of polymers in platelet growth and to maintain the procedures of Hg12 crystal growth by vapor. In 1980, a study conducted by S.P. Faile et al. concluded that the use of polymers, specifically polyethylene, within the growth ampoule induced platelet growth. Since then, the incorporation of polymers in platelet growth has been widely employed; however, the role of polymers in platelet growth is not conclusive. Systematic experiments were carried out to determine the appropriate combination of furnace end temperature, temperature gradient, and the amount of polymers required to grow platelets of usable size. Comparison of crystal properties between crystals grown with the vertical and horizontal methods was made.

DTRA-TR-13-7, Control of Grain Boundaries and Defects in Nano-Engineered Transparent Scintillator Ceramics

This research program focused mainly on the relationship between macro-scale defects on the scintillator properties of optical ceramics. The formers include grain boundaries, porosity and solid phase inclusions, and the latter, lattice imperfections. The following important results were found: (1) Oxygen defects in hot pressed Eu-doped yttrium oxide ceramics dwarf the influence of grain boundary defects on scintillator light yield (5 to 250 micron grain size range). A direct relationship was found between the in diffusion of oxygen during annealing and the decrease in the number of charge carrier traps. This oxygen uptake resulted in an increased in light yield. (2) Two novel micro-sale scintillation characterization techniques were developed. (3) Grain boundary recombination is Eu-doped yttrium oxide ceramics was found to be minimal. Transmission electron microscopy showed that these ceramics had abrupt boundaries. (4) In vacuum sintered Ce-doped yttrium aluminum garnet ceramics, a relationship was found between cation non-stoichiometry, anti-site defects, and light yield. (5) In translucent Eu-doped strontium iodide ceramics produced by hot pressing, a relationship between transparency, grain texture and scintillation properties was identified.

DTRA-TR-13-8, Strategy for Enhanced Light Output from Luminescent Nanoparticles

The objective of this research program was to synthesize luminescent oxide or halide nanoparticles with improved brightness and scintillation efficiency under excitation by energetic x-ray and gamma radiation. Improved brightness and efficiency was achieved by growth of undoped and doped nanoparticles with a core/shell nanostructure. The nanoparticle properties characterized included photoluminescence-PL, crystallography, particle size distribution, quantum efficiency, and nuclear spectroscopic responses.

DTRA-TR-13-10, Engineering Methodology Report, Component Vulnerability Module Integrated Munitions Effects Assessment (IMEA) Underground Targeting and Analysis System (UTAS)

The Component Vulnerability Module (CVM) assesses the vulnerability (or fragility) of equipment. We define equipment as items added to the target models that are not part of the building or tunnel structure but rather carry out a mission or function important to the operation of the target. For example, a generator is an equipment item, but a column is not. The need to address the functional defeat of targets and target systems requires assessment of the vulnerability of individual equipment items. The CVM is responsible for these assessments. The model uses data-driven equipment descriptions and calculated weapon-environment properties to estimate equipment vulnerability.

DTRIAC Collection Additions *(continued)*

DTRA-TR-13-11, Engineering Methodology Report, Threat and Structure Iso-Damage Contour Module, Vulnerability Assessment and Protection Option Version 5.1

The Threat and Structure Iso-Damage Contour Module (DCM) creates a component module to display contours of constant damage around an explosive threat source and structures. These contours show safe standoff distances from an explosive charge for expedient vulnerability assessment of personnel and building damage for various levels of damage. These contours permit "what-if" scenarios based on simple, straight-line, Kingery-Bulmash airblast calculations. P-I level fidelity damage models, and fragility functions. The component provides contouring capabilities that are commensurate with existing damage visualization capabilities (AT Planner and BEEM); the exception being that the software application provides the option for threat-centric damage contouring for any modeled building.

DTRA-TR-13-12, Engineering Methodology Report, Nuclear Contours, Vulnerability Assessment and Protection Option Version 5.1

The Effects Manual One (EM-1) Technical Handbook contains equation, tables, and figures for phenomena resulting from a nuclear detonation and the resulting effects to buildings and human personnel. This data will be used to create curves of the relationship between yield and the range to a given effect. The curves will be fit to generate equations that will be implemented in code.

DTRA-TR-13-14, Engineering Methodology Report, Site Attack Module Vulnerability Assessment and Protection Option Version 5.1

The Site Attack Module provides the capability to calculate airblast pressure and impulse from a single explosive number of buildings. The module takes into consideration the first surface reflection, the three-dimensional shielding from other structures, and the dispersion of the blast pressure around obstructions. The engineering methodology for the Site Attack Model is composed of two sub-modules, which are the Site Preparation Module and the Site Airblast Module. The Site Preparation Module creates a faceted representation of the modeled site. This faceted representation is a 3D region limited by the terrain and the building exterior surfaces, including berming. The module makes the faceted representation available to other modules for airblast computation as well as to the Site Post Calc Module for possible display of the faceted model in the GUI 3D view.

DTRA-TR-13-15, Engineering Methodology Report, Structural Elements Module, Vulnerability Assessment and Protection Option Version 5.1

The Structural Elements Module (SEM) creates new, XML-driven component modules for pressure-impulse (P-I) damage functions, response surface (RS) damage functions, and single-degree-of-freedom (SDOF) response models. Several new models to predict damage of non-retrofit and retrofit structural elements are introduced. We group these new models based on input–output similarities. We implement each group in independent, extensible, data driven modules. The SEM implements the range-to-effect curves for CMU wall retrofits published by the US Army Corps of Engineers (USACE) in ETL 1110-3-494, Airblast Protection Retrofit for Unreinforced Concrete Masonry Walls (10). The ETL provides guidance for the retrofit upgrades existing, unreinforced, non-load bearing, concrete, masonry walls to provide protection against airblast.

DTRA-TR-13-16, Engineering Methodology Reports, Vehicle Routes and Barriers Vulnerability Assessment and Protection Option Version 5.1

The Vehicle Barrier Selection (VBS) component assists the user in selecting anti-ram vehicle barriers for facility protection. The VBS component implements the methodology for barrier selection per the Unified Facilities Criteria (UFC) document 4-022-02 (2). This and all other UFC documents are maintained by the United States Army Corps of Engineers (HQUSACHE), Naval Facilities Engineering Command 9NAVFAC), and Air Force Civil Engineer Support Agency (AFCESA) per MIL-STD-3007. This component updates and replaces the Vehicle Barrier Ramming component that was based on an earlier methodology.

DTRA-TR-13-17, Methodology Overview, Vulnerability Assessment and Protection Option, Version 5.1

This document is part of the VAPO project documentation suite. This document summarizes the list of the Methodology Reports and Design Documents that are applicable to VAPO. We describe new major features of VAPO in the Software Version Description (SVD) [1]. We deliver this document toward the end of the version to ensure it contains a list of all VAPO version functionality. VAPO is a fast-running software tool, able to operate on notebook computers and model the effects of a wide range of events. The software leverages existing government owned products to the greatest extent possible. The code is easy to expand for new threats or better models.

DTRA-TR-13-18, Task 14, Develop CZT Crystal Gamma-Ray Spectrometer

This study was a direct follow-on to the Defense Threat Reduction Agency (DTRA) Task 3 for the study of cadmium zinc telluride (CZT) crystals and the development of a gamma-ray spectrometer system. The CZT crystals evaluated under DTRA Task 3 did not provide the requisite spectral response to justify further study or the design of the spectrometer system.

DTRA-TR-13-19, Cycle 6 Test and Evaluation, Report on the Continuing Evaluation of Radioisotope Identifiers (RIIOs)

The Cycle 6 RIID testing and evaluation occurred over 10 months, utilizing 17 commercial instruments. This cycle continued to stress the systems in configurations likely encountered by DoD users. A new element of this cycle was analysis of a limited set of RIID data by a JTOT triage/reachback team. The results clearly indicated the challenges of correctly identifying SNM, the added complexity introduced by shielding and masking to a single SNM, and the greater difficulty in identifying multiple sources. Cycle 6 results also indicated notable improvements in a number of instruments, including the ORTEC HX, FLIR Raider, and BNC SAM-940-Nal.

DTRA-TR-13-20, Experimental Research in Advanced Concepts for Novel Reactive Materials

This proposed research addressed two areas of reactive materials (RM) research that can potentially improve DoD capabilities for defeat of WMDs. The first concept seeks to enhance feasibility of weaponizing RMs by researching a novel route to the production of metal-matrix composite RM casings and liners-infiltration of dense inert fibrous grids (e.g., W wire) with castable lighter energetic metals (e.g., Al). This approach would potentially yield a route to practical, cost-effective production of nonporous, highly energetic, high-density RM liners and cases with high strength

DTRIAC Collection Additions *(continued)*

and stiffness. Such an approach would be a great improvement in cost over the powder-based techniques currently envisioned—greatly speeding implementation.

DTRA-TR-13-21, NWF1RES: Fire Ignition and Propagation Code for Near Surface Weapons Effects Tools 3D (NSWET-3D)

NWFIRES is a comprehensive fire assessment code integrating state-of-the-art algorithms for fire-start and fire-spread as they result from a nuclear detonation of user-defined yield and location. After calculating the thermal radiation output from the nuclear fireball and the airblast overpressure and time of shock arrival from the detonation, NWFIRES models the initial fires that develop in the immediate area. Primary fires result from direct or indirect exposure of ignitable fuels to the fireball thermal radiation. Fires that develop as a result of blast disruption of structures and their contents (e.g., overturned heating appliances and gas line ruptures) are classified as secondary fires. Spread of initial fires is calculated using a historical/statistical spread model. During the 12-month option of the NSWET-3D program we performed the following: initiated a transition of NWFIRES from the original DFAD occupancy/land-use database to the more current census-based HAZUS database; updated NWFIRES to import building damage levels from Weidlinger's (WAI) structural calculations within NucFast; and changed the input format from user-interactive to imported input file.

DTRA-TR-13-22, Report on the Findings from the 2012 DTRA Fundamental Research Thrust Area 6: "Cooperative Counter-WMD with Global Partners" Annual Programmatic & Technical Review

The Defense Threat Reduction Agency Research and Development's Basic and Applied Sciences department (J9-BA) hosted the second annual programmatic and technical review for fundamental research projects funded under the auspice of Thrust Area 6: Cooperative Counter Weapons of Mass Destruction (WMD) Research with Global Partners. The review was held 5–7 November 2012 at the National Academy of Sciences in Washington, D.C. The purpose of the review was to evaluate success of collaborative efforts and congruence with Cooperative Biological Engagement Program (CBEP) objectives and to assess technical progress of currently funded projects.

DTRA-TR-13-23, Synthesis, Characterization, and Multimillion-Atom Simulation of Halogen-based Energetic Materials for Agent Defeat

The previously unknown I207 was successfully synthesized and characterized. The only missing piece of information is a crystal structure. It was shown that it is of insufficient thermal stability, but that the known I206 is an excellent substitute. The literature synthesis for I206 was drastically improved and scaled up to the 100 g level. Several hundred grams of I206 were prepared and provided to Professor Vashistha (USC), Professor Dreizin (NM Inst. Of Technology), Professor Zachariah (U of Maryland), Dr. Higa (NAVAIR, Chinal Lake), Dr. Lightstone (Indian Head), Dr. Liu (NIST) and Dr. Kolesnikov (Oakridge) for further evaluation. Explosives testing at NAVIAR and Indian Head, powder diffraction measurements at NIST and neutron diffraction and inelastic scattering experiments at Oakridge have been highly successful. At the suggestion of Dr. Su Peiris, coating studies for I206 were also carried out which resulted in an improvement of its hydrolytic stability. First-principle quantum-mechanical calculations of I205 and I206 crystals were carried out to investigate their structural and lattice-dynamic properties. Their equations of states and thermodynamic properties at high pressures and temperatures were also calculated.

DTRA-TR-13-26, A Fast Running Rad-Hydro Program for Simulations of Nuclear Weapon Portal Attack on Tunnel Targets

This report details the development of a fast running rad-hydro program to analyze the effects of a portal attack with a low yield nuclear device on a representative tunnel complex. The primary objective of this work was the development of an intuitively east GUI tool to allow a user to rapidly set up and simulate a portal attack. Special modifications to the SAGE/RAGE rad-hydro code were made to accommodate the calculations.

DTRA Small Business Innovation Research

SBIR C11-01, A Novel Cost effective Method for Growing High Performance Radiation Sensors

SBIR Phase I Report, Radiation Effects Characterization Tool for SiGe Processes

DTRA Internal Reports

DTRA-IR-13-28, Teller Light Transport

This Quarter in History

April 1939 — A secret uranium research project was established in Germany, taking steps to explore possible military uses of uranium fission. A ban on the export of uranium is imposed to ensure enough material for the project.

May 25, 1953 — UPSHOT-KNOTHOLE GRABLE was the first test of an artillery-fired atomic projectile (AFAP). The device was launched from a special 280-mm cannon and detonated over 11,000 yards away.

May 18, 1974 — India detonates its first atomic bomb, SMILING BUDDHA, with yield estimates up to 8 kT. India had begun its nuclear program in 1944.

Modeling Nuclear Blast in Urban Terrain with NucFast *(continued)*

Applying these methods to an urban scene yields results consistent with first-principles calculations of building loads. NucFast uses GIS-based scenes with buildings developed using light detection and ranging (LIDAR) data. The airblast environment is predicted at ground level and on all building surfaces. Parameters such as peak overpressure, peak dynamic pressure, and associated impulse can be overlaid onto the scene in 2D or 3D (Figure 4).

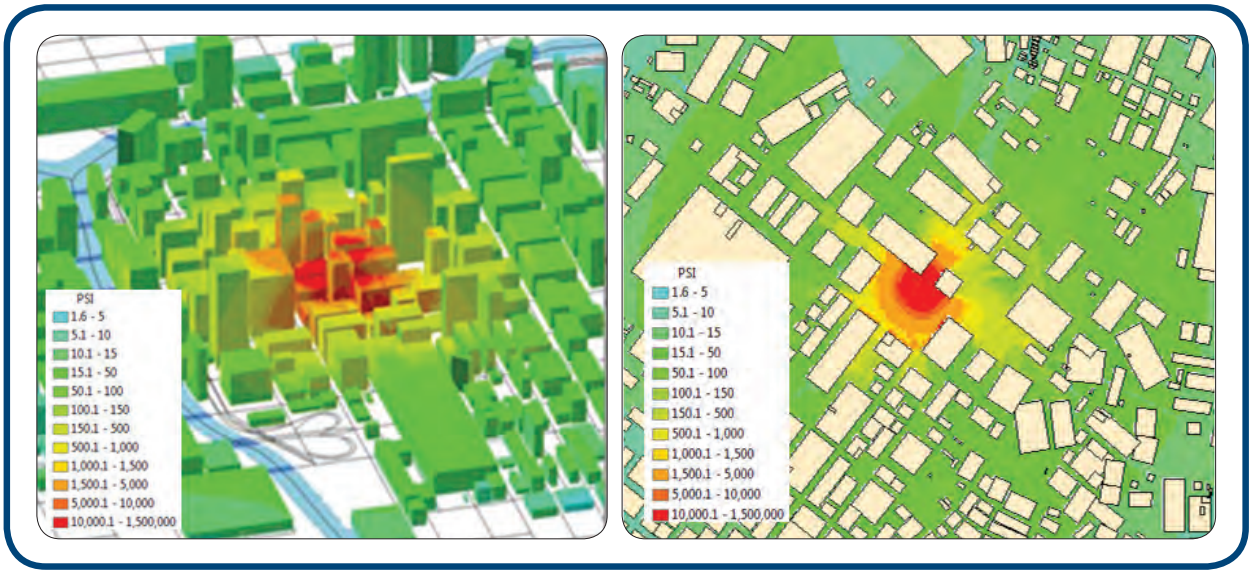

Figure 4. NucFast 2D and 3D output of peak overpressures located on building and ground surfaces (ARA, Inc.)

References

1. Needham, C. E. and J. E. Crepeau, "The DNA Nuclear Blast Standard (1 KT)," DNA 5648T, prepared by S-Cubed for the Defense Nuclear Agency, Alexandria, Virginia, January 1981 (UNCLASSIFIED).

2. Hikida, S. and C. E. Needham, "Low Altitude Multiple Burst (LAMB) Model, Volume I - Shock Description," DNA 5863Z-1, Defense Nuclear Agency, Washington, D. C., 30 June 1981 (UNCLASSIFIED).

Ask the IAC

How Do I Get My Report Loaded Into STARS?

DTRIAC accepts all types of scientific and technical information (STINFO) of enduring historical value to DTRA and its missions. These materials can be provided in any format (hard copy documents, CDs, DVDs, films, videos, photographs, etc.) and can include classified or unclassified data.

Getting DTRA reports into the Scientific and Technical Information Archival and Retrieval System (STARS) has never been easier. Simply notify the DTRIAC Documents Area Manager at (505) 846-9420 to make arrangements to submit the technical reports. Once your documents are received at DTRIAC, an item number is assigned and a cataloged citation is created on STARS. These searchable cataloged entries will include title, classification, caveats, distribution statements, abstracts, media type, and descriptors. Your document is then digitized and a searchable pdf file is created to be added to the STARS citation. To retrieve your document on STARS, simply click the highlighted link in the citation to open up the pdf file.

Many documents are submitted to DTRIAC on CDs that contain a pdf file of the report. This streamlines the process, guarantees the integrity of the data, and expedites access to your documents. Agency reports are generally loaded and accessible on STARS within 24 to 48 hours of receipt.

Should you have questions on how to send photos, film, videos, and other media types with your agency report, please contact the DTRIAC Media Manager at (505) 846-4494.